

RBP2 is an MRG15 complex component and down-regulates intragenic histone H3 lysine 4 methylation

Tomohiro Hayakawa¹, Yasuko Ohtani¹, Noriyo Hayakawa¹, Kaori Shinmyozu², Motoki Saito³, Fuyuki Ishikawa³ and Jun-ichi Nakayama^{1,*}

¹Laboratory for Chromatin Dynamics, and

²Proteomics Support Unit, Center for Developmental Biology, RIKEN, Kobe, Hyogo 650-0047, Japan

³Laboratory for Cell Cycle Regulation, Department of Gene Mechanisms, Graduate School of Biostudies, Kyoto University, Kitashirakawa-Oiwake-cho, Sakyo-ku, Kyoto 606-8502, Japan

MRG15 is a conserved chromodomain protein that associates with histone deacetylases (HDACs) and Tip60-containing histone acetyltransferase (HAT) complexes. Here we further characterize MRG15-containing complexes and show a functional link between MRG15 and histone H3K4 demethylase activity in mammalian cells. MRG15 was predominantly localized to discrete nuclear subdomains enriched for Ser²-phosphorylated RNA polymerase II, suggesting it is involved specifically with active transcription. Protein analysis of the MRG15-containing complexes led to the identification of RBP2, a JmjC domain-containing protein. Remarkably, over-expression of RBP2 greatly reduced the H3K4 methylation in culture human cells *in vivo*, and recombinant RBP2 efficiently removed H3K4 methylation of histone tails *in vitro*. Knockdown of RBP2 resulted in increased H3K4 methylation levels within transcribed regions of active genes. Our findings demonstrate that RBP2 associated with MRG15 complex to maintain reduced H3K4 methylation at transcribed regions, which may ensure the transcriptional elongation state.

Introduction

Histone N-terminal tails are subjected to multiple covalent modifications that affect chromatin structure and transcription (Strahl & Allis 2000). Histone acetylation at lysine residues is closely linked to active transcription and is dynamically controlled by histone acetyltransferases (HATs) and histone deacetylases (HDACs). Most of the HATs and HDACs are part of large multiprotein complexes, whose subunits mediate regulation, recruitment, substrate recognition and other undefined functions. While histone acetylation is dynamically regulated by balancing the opposing activities of HATs and HDACs, histone lysine methylation serves as an additional stable epigenetic mark, participating in a variety of biological processes, including both transcriptional activation and repression (Lachner & Jenuwein 2002). Recent studies suggest that histone lysine methyl groups are removed by at least two distinct classes of enzymes: the nuclear amine oxidase homologs and the JmjC-domain proteins. LSD1

belongs to the first of these classes and was the first histone lysine demethylase identified; it specifically demethylates methylated histone H3 lysine 4 (H3K4me) (Shi *et al.* 2004). Unlike LSD1, which can only remove mono- and dimethyl lysine modifications, the JmjC-domain-containing histone demethylases (JHDMs) can reverse all three mono-, di- and tri-methylation states. It has been shown that JHDM1 and JHDM2A possess demethylase activity specific to H3K36me and H3K9me, respectively, and that JHDM3 demethylates both H3K9me and H3K36me (Klose *et al.* 2006).

Human MRG15 and MRGX were originally identified as factors closely related to MORF4 (mortality factor on human chromosome 4), whose transient expression induces senescence in a subset of human tumor cell lines (Bertram *et al.* 1999). Although these proteins show extensive sequence similarities and share common motifs such as helix-loop-helix and leucine zipper regions, only MRG15 contains an N-terminal chromodomain and has known orthologs in other eukaryotic species, suggesting MRGX and MORF4 emerged late in evolution (Bertram & Pereira-Smith 2001). In the budding yeast *S. cerevisiae*, the MRG15 homologue Eaf3 is a component of both the

Communicated by: Fumio Hanaoka

*Correspondence: E-mail: jnakayam@cdb.riken.jp

DOI: 10.1111/j.1365-2443.2007.01089.x

© 2007 The Authors

Journal compilation © 2007 by the Molecular Biology Society of Japan/Blackwell Publishing Ltd.

Genes to Cells (2007) 12, 811–826

811

NuA4 HAT and Rpd3 HDAC complexes and functions in transcriptional regulation (Eisen *et al.* 2001; Gavin *et al.* 2002). We previously showed that the fission yeast homologue, Alp13, is a component of the Clr6 HDAC complex and is required for the maintenance of genome integrity (Nakayama *et al.* 2003). Human MRG15 has also been identified as a stable component of both the Tip60 HAT (NuA4) and HDAC complexes (Yochum & Ayer 2002; Cai *et al.* 2003; Doyon *et al.* 2004). Together, these results implicate MRG15 family proteins in modulating histone acetyl modification for both transcriptional regulation and DNA double-strand break (DSB) repair (Doyon & Cote 2004; Kusch *et al.* 2004).

Several lines of evidence suggest that human MRG15 and MRGX are involved in both the activation and repression of transcription. MRG15 and MRGX interact with RB in nucleoprotein complexes and activate or repress β -Myb promoter activity in a cell-type-dependent manner (Leung *et al.* 2001; Tominaga *et al.* 2003). MRG15 also interacts with the mSin3 co-repressor complex, and the tethering of MRG15 to the promoter region leads to the repression of a reporter gene (Yochum & Ayer 2002). Recent studies on *Mrg15*-deficient mice revealed that the mice die as embryos and have a reduced number of proliferating cells (Tominaga *et al.* 2005a). Although *MrgX*-null mice have no detectable phenotype, analysis of *Mrg15*^{-/-}, *MrgX*^{-/-} double-null embryos suggested that *Mrg15* and *MrgX* have overlapping functions in early embryogenesis (Tominaga *et al.* 2005b).

Promoter and transcribed regions at active gene loci are marked by characteristic patterns of histone acetylation and methylation (Millar & Grunstein 2006). The recruitment of HATs to specific promoter regions facilitates gene expression, and a global pattern of histone H3 and H4 acetylation is created in which the levels are generally high in promoter and low in transcribed regions. Recent studies on *S. cerevisiae* revealed that transcriptional initiation and transcribed regions are differentially marked by H3K4 and H3K36 methylation, which are mediated, respectively, by Set1 and Set2 methyltransferases (Hampsey & Reinberg 2003). Moreover, these modifications are mechanistically connected to the phosphorylation state of the carboxy-terminal domain of RNA polymerase II. In *S. cerevisiae*, the loss of Eaf3, the homologue of MRG15, causes an increase in histone H3 and H4 acetylation within transcribed regions (Reid *et al.* 2004). Preferential deacetylation at transcribed regions is considered to suppress intragenic transcription initiation (Kaplan *et al.* 2003). Further studies revealed that Eaf3 interacts with H3K36me through its chromodomain and recruits Rpd3S, one of the Rpd3-containing complexes, to H3K36-methylated nucleosomes, that leading to the

deacetylation of transcribed regions (Carrozza *et al.* 2005; Joshi & Struhl 2005; Keogh *et al.* 2005). Although these studies implicate the MRG15 family proteins in transcriptional elongation, the exact mechanisms by which human MRG15 and its related proteins function in this process have remained elusive.

Here we report the biochemical characterization of MRG15-associated complexes and show that the JmjC-domain protein, RBP2 (also known as JARID1A), specifically interacts with the MRG15 complex. We further show that the over-expression of RBP2, but not a catalytically inactive mutant, reduces the H3K4 tri-, di- and mono-methylation levels in human cultured cells. Finally, we demonstrate that the RNAi depletion of RBP2 results in increased H3K4 methylation at the transcribed regions of active genes. These results suggest that MRG15-containing complexes target H3K36me-enriched transcribed regions and further recruit the H3K4 demethylase, RBP2 and HDAC complexes.

Results

MRG proteins localize to nuclear subdomains associated with active transcription

Although recent studies on *S. cerevisiae* uncovered a specific role for Eaf3 in maintaining the hypoacetylation at transcribed regions, the precise role of human MRG15 and its related proteins (MRGX, a highly homologous protein lacking the N-terminal chromodomain; and MRGBP, a tightly associated partner protein) in transcriptional regulation is incompletely understood. To probe the function of MRG proteins in transcriptional regulation, we first analyzed their subcellular localization in human cell lines using polyclonal antibodies raised against each recombinant protein. These antibodies specifically recognized endogenous proteins and no cross-reactive bands were observed in Western analysis (data not shown). MRG15 was distributed throughout the nucleoplasm in formaldehyde-fixed HeLa cells (Fig. 1A, formaldehyde); a similar nucleoplasmic distribution was observed for transiently-expressed GFP-MRG15 protein in living cultured cells (data not shown). If the cells were fixed with methanol, the MRG15 signals were detected as dozens of nuclear foci resembling "splicing speckles" with nucleoplasmic distribution (Fig. 1A, methanol). These MRG15 signals were largely excluded from chromatin regions intensely stained with DAPI (Fig. 1A, merge). Similar fixation-dependent distribution was observed for MRGX and MRGBP, and their signals in methanol-fixed cells overlapped with those of MRG15, partly for MRGX and more so for MRGBP (Fig. 1B,C).

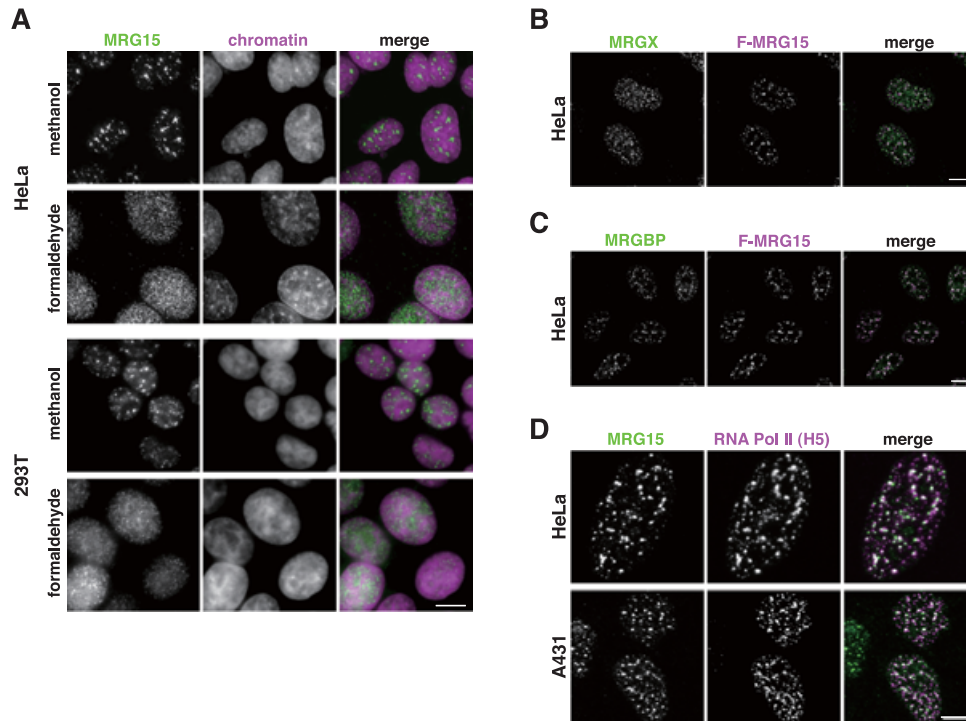


Figure 1 MRG15 localizes to the transcriptionally active nuclear domains. (A) Immunofluorescence images of HeLa (upper) and 293T (lower) cells. Cells were fixed with cold methanol (upper row) or formaldehyde (lower row) followed by indirect immunostaining using an anti-MRG15 antibody (left column). Chromatin was visualized by DAPI (middle column), and merged images of the green (MRG15) and magenta (chromatin) staining are shown in the right column. Overlapped signal of the green and magenta becomes white. (B, C) Immunofluorescence images of HeLa cells expressing FLAG-tagged MRG15 (F-MRG15). Cells were fixed with cold methanol, followed by immunostaining with an anti-MRGX or MRGBP antibody (left) or anti-FLAG M2 antibody for F-MRG15 (middle). Merged images of green (MRGX or MRGBP) and magenta (MRG15) staining are shown on the right. (D) Immunofluorescence images of HeLa (upper) and A431 (lower) cells. Cells were fixed with cold methanol and then stained using anti-MRG15 (left column) and anti-RNA Pol II (H5) antibodies (middle column). Merged images of the green (MRG15) and magenta (RNA Pol II) staining are shown in the right column. Scale bar, 10 μ m.

These localization patterns were confirmed in different cell types, including human HEK293T, A431 and mouse NIH3T3 cells (Fig. 1A and data not shown). One interpretation of these data is that the nucleoplasmic distribution exhibited following different fixation conditions represents distinct subfractions of MRG15.

Hyperphosphorylated RNA polymerase II exhibits fixation-dependent distribution analogous to that of MRG proteins (Bregman *et al.* 1995; Guillot *et al.* 2004). To gain further insight into the relationship between MRG15 and transcription, we investigated whether MRG15 foci co-localized with signals for RNA polymerase II and histone methyl modifications associated with active transcription. RNA polymerase II engaged in transcriptional elongation step is hyperphosphorylated on Ser² of its C-terminal domain and is specifically recognized in this state by monoclonal antibody, H5 (Bregman *et al.* 1995; Guillot *et al.* 2004). Immunostaining of RNA poly-

merase II using this antibody exhibited a punctate nuclear distribution in methanol-fixed HeLa cells that resembled that of MRG15 (Fig. 1D; Guillot *et al.* 2004). Indeed, these RNA polymerase II signals preferentially co-localized with those of MRG15 (Fig. 1D). Moreover, MRG15 signals also overlapped with those of H3K4me3 and H3K36me3 (Supplementary Fig. S1A, S1B). Taken together, these results suggest that the MRG15-enriched nuclear subdomains are associated with the sites of active transcription, and further support the idea that MRG15—and presumably MRGX and MRGBP—play a critical role in the transcriptional elongation.

Characterization of MRG15-, MRGX- and MRGBP-containing complexes

Human MRG15 is known to be a component of both the Tip60 HAT and HDAC complexes (Yochum & Ayer

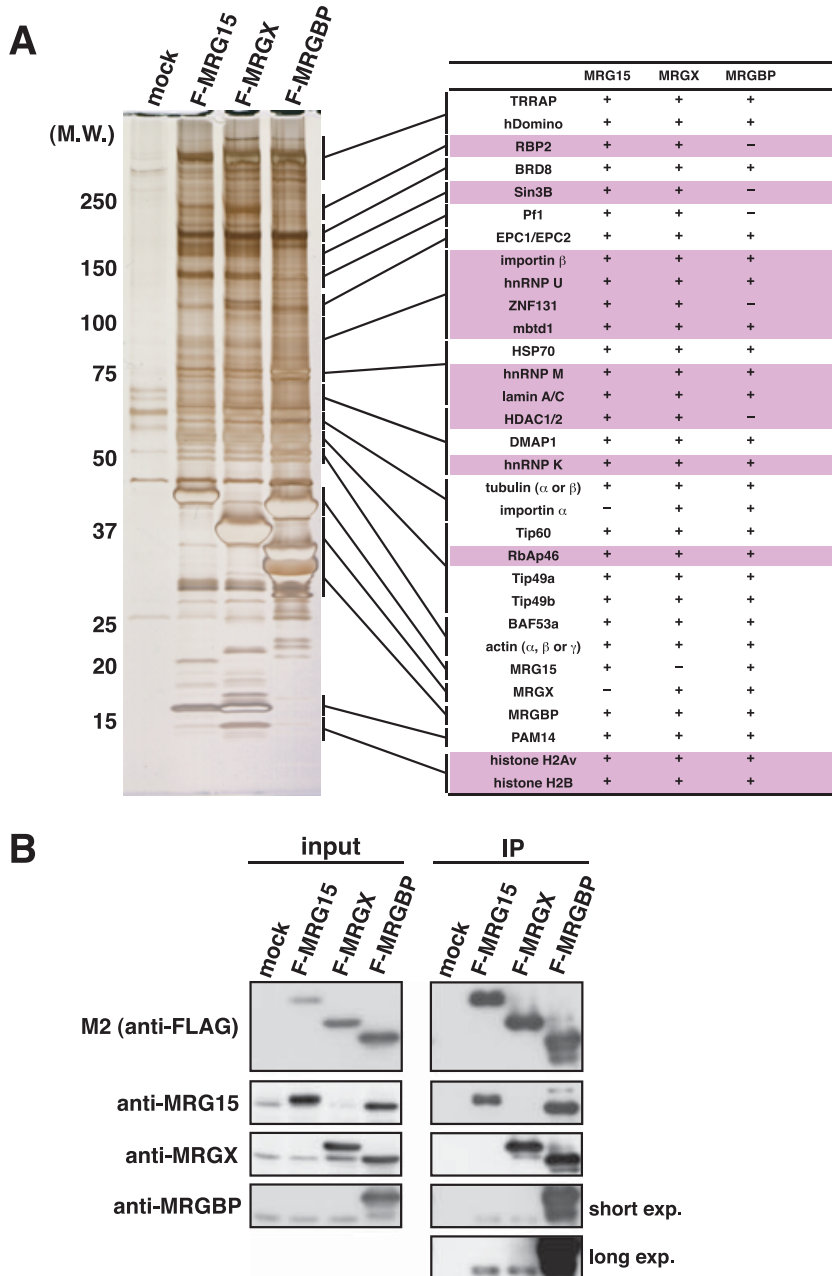


Figure 2 Immunoaffinity purification of MRG protein complexes. (A) Affinity-purified MRG15-, MRGX- and MRGBP-complexes from HeLa cells were subjected to 4%–20% SDS-PAGE followed by silver staining (left). Each protein band was excised from the gel and subjected to LC-MS/MS analysis. Interacting proteins identified by LC-MS/MS analysis are indicated on the right. Newly identified proteins are highlighted in pink. Mock indicates the purification results using cells transformed with an empty expression vector. (B) MRG15 and MRGX form distinct complexes that are mutually exclusive. Nuclear lysates (input) of HeLa cells expressing each of the FLAG-tagged MRG proteins and immunoprecipitated fractions (IP) using anti-FLAG M2 agarose, were subjected to Western blot analysis using specific antibodies to the MRG proteins. Bands in the mock lane of input indicate endogenous MRG proteins.

2002; Cai *et al.* 2003; Doyon *et al.* 2004), but neither its specific role in these complexes nor the relationships with MRGX or MRGBP are clear. To investigate the distinctive functions of the MRG family proteins, we purified and analyzed MRG15-, MRGX- and MRGBP-containing complexes. We produced HeLa cell lines that expressed N-terminal FLAG-tagged fusions (F-MRG15, F-MRGX or F-MRGBP) in a tetracycline-regulated manner. The lines were subjected to immune affinity

chromatography using anti-FLAG antibodies and purified proteins were analyzed by SDS-PAGE (Fig. 2A) and Western blotting using cognate antibodies (Fig. 2B). The profiles of the F-MRG15- and F-MRGX-associated complexes were largely superimposable (Fig. 2A), although F-MRG15-associated complexes did not include native MRGX or vice versa (Fig. 2B, IP). These results suggest that MRG15 and MRGX are mutually exclusive to complexes with an otherwise similar composition. Since

MRGX lacks a chromodomain, this further indicates that the chromodomain is not required for complex formation. The profile of the F-MRGBP-associated proteins was similar to that of F-MRG15 and F-MRGX (Fig. 2A), and native MRG15 and MRGX were present in the F-MRGBP-precipitated fraction (Fig. 2B, IP). This result is consistent with previous observations (Cai *et al.* 2003) and suggests that MRGBP is a shared component of MRG15- and MRGX-containing complexes. Interestingly, we noticed that the expression of F-MRGBP caused an increase in the protein levels of MRG15 and MRGX (Fig. 2B, input, F-MRGBP). This result implies that MRGBP plays a role in regulating synthesis and/or stability of MRG15 and MRGX.

RBP2 is associated with MRG15- and MRGX-containing complexes

To investigate further the composition of MRG15- and MRGX-containing complexes, each constituent band following SDS-PAGE was excised and analyzed by nano-liquid chromatography tandem mass (LC-MS/MS) spectrometry. This analysis detected most of the proteins previously identified as being associated with MRG15 or MRGBP (Cai *et al.* 2003; Doyon *et al.* 2004) and confirms that MRG15- and MRGX-containing complexes are associated with both Tip60 HAT- and HDAC-associated factors (Fig. 2A). However, our analysis also revealed several novel proteins, including the retinoblastoma (RB) binding protein RBP2, ZNF131, Mbt domain containing 1 (MBTD1), hnRNP K, hnRNP M and hnRNP U, stably associated with MRG15- or MRGX-containing complexes (Fig. 2A, highlighted in pink). Although any functional link between these newly identified factors and MRG proteins remains to be shown, this observation forms a physical basis for the functional correlation between MRG15 and RBP2-mediated transcriptional regulation (Kim *et al.* 1994; Chan & Hong 2001; Benevolenskaya *et al.* 2005). In addition, RBP2 possesses a conserved JmjC domain, recently shown to correspond to the catalytic domain of histone demethylase (Klose *et al.* 2006), implying that it could be involved in the dynamics of histone methyl modifications. Therefore, we focused on RBP2 and its relationship with MRG proteins and transcriptional regulation.

We first analyzed their association by gel filtration chromatography. MRG15, MRGX and MRGBP in HeLa nuclear extract were eluted with distinct profiles and part of them was detected in fractions corresponding to more than 600 kDa (Fig. 3A). RBP2 and HDAC2 were also eluted in fractions for higher molecular weight. These results suggest that MRG15, MRGX and MRGBP are

a component of large protein complexes and their elution profiles were overlapped with that of RBP2. To assess in greater detail the specificity of interaction between RBP2 and the MRG proteins, we performed immunoprecipitation (IP) of F-MRG proteins and analyzed precipitated RBP2 by Western blotting using an anti-RBP2 antibody. We found that RBP2 interacted with F-MRG15 and F-MRGX, but not with F-MRGBP (Fig. 3B). Similar specificity was observed for Sin3B and HDAC2. This was consistent with our LC-MS/MS analysis, in which no RBP2, Sin3B or HDAC2 peptide was detected in the F-MRGBP-precipitated fraction (Fig. 2A). These results suggest that MRG15 and MRGX are components of distinct HAT and HDAC complexes and that RBP2 specifically associated HDAC complexes containing either MRG15 or MRGX. MRGBP appeared to be specific to Tip60-containing HAT complexes (Figs 2A and 3B), in good agreement with the identification of Eaf7, an MRGBP homolog in *S. cerevisiae*, in NuA4 HAT, but not in Rpd3-containing HDAC complexes (Krogan *et al.* 2004). Under the conditions of these IP Westerns, the level of interacting RBP2 was relatively higher in the F-MRG15-precipitated fraction than in that of F-MRGX (Fig. 2B, RBP2). To corroborate this pattern of specificity, we expressed N-terminal FLAG-tagged RBP2 (F-RBP2) in HeLa cells. F-RBP2-associated proteins were isolated from nuclear extracts by immunoprecipitation and identified by Western blotting (Fig. 3C,D). This revealed that F-RBP2 belonged to stable complexes containing MRG15, Sin3B and HDAC2 (Fig. 3C), but not Tip60, MRGX or MRGBP (Fig. 3D). Together, these reciprocal IP-Western experiments further demonstrate that, although RBP2 was detected in co-immunoprecipitates containing either F-MRG15 or F-MRGX (Figs 2A and 3A), it preferentially associates with the MRG15-containing HDAC complex.

RBP2 over-expression induces histone H3K4 demethylation *in vivo*

We next examined the subcellular localization of RBP2. Since the anti-RBP2 antibody was not applicable to immunostaining, due to its high background, we examined RBP2 localization using HeLa cells that stably expressed tetracyclin-regulated F-RBP2. F-RBP2 in HeLa cells predominantly localizes to discrete nuclear foci and partially co-localized with MRG15 or Ser²-phosphorylated RNA polymerase II (Fig. 3E,F), suggesting its involvement with transcriptional regulation. MRG15 binds H3K36-methylated histone tail (Zhang *et al.* 2006) and it is therefore suggested that MRG15 plays a role in transcribed regions to recruit the HDAC

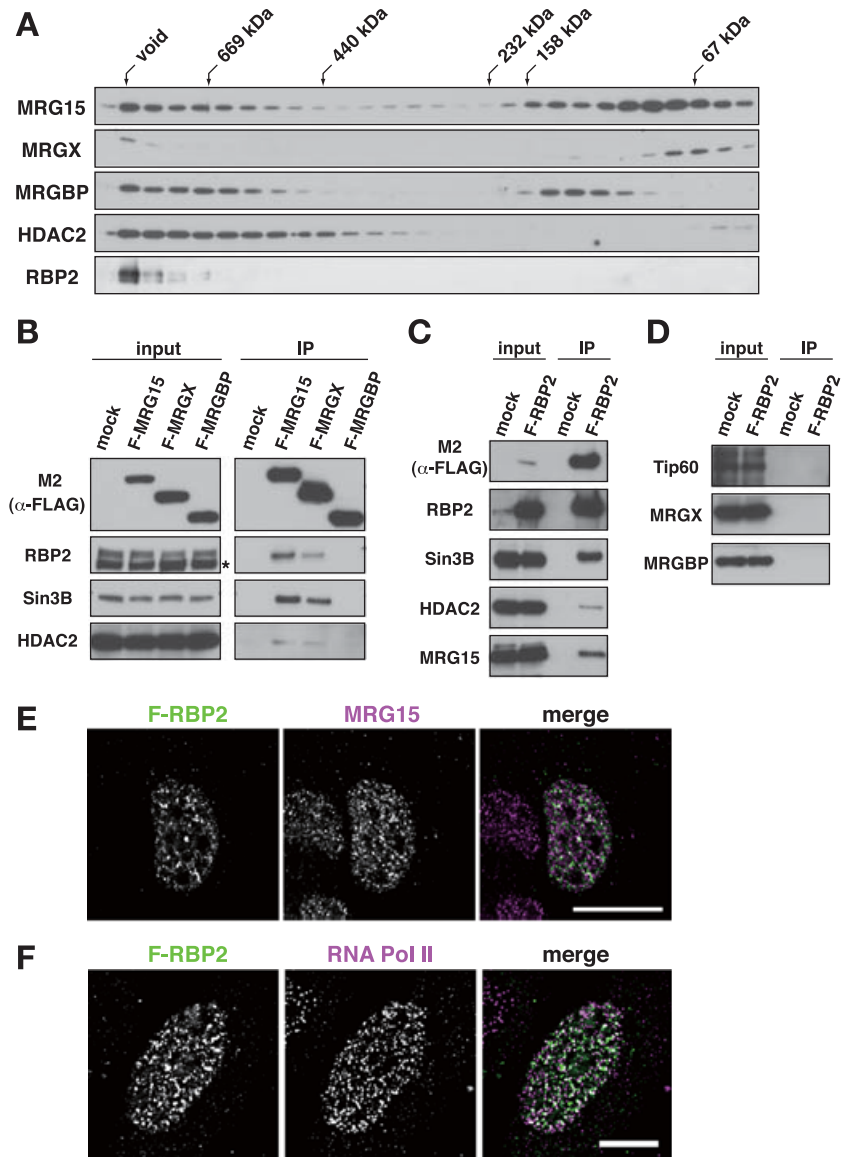
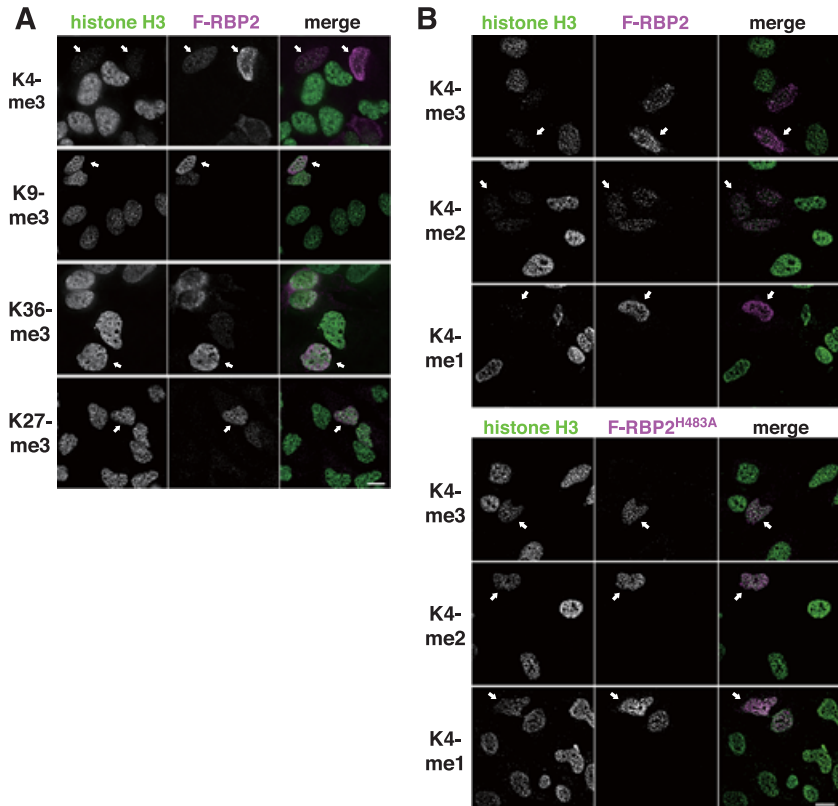


Figure 3 RBP2 interacts with the MRG15-containing HDAC complex. (A) Nuclear extract prepared from HeLa cells was fractionated on a Superdex 200 gel filtration chromatography and analyzed by Western blot using polyclonal antibody against MRG15, MRGX, MRGBP, HDAC2 or RBP2. Bovine serum albumin (67 kDa), aldolase (158 kDa), catalase (232 kDa), ferritin (440 kDa) and thyroglobulin (669 kDa) were used for molecular mass standards. (B) RBP2 interacts with MRG15 and MRGX complexes, but not with the MRGBP complex. Nuclear lysates (input) of HeLa cells expressing each of FLAG-tagged MRG proteins and immunoprecipitated fractions (IP) using anti-FLAG M2 agarose were subjected to Western blot analysis using an anti-RBP2, anti-Sin3B or anti-HDAC2 antibody. Mock indicates the purification results using HeLa cells transformed with an empty expression vector. Asterisk indicates non-specific protein bands. (C, D) RBP2-associated proteins were immunoprecipitated from HeLa cells expressing FLAG-RBP2. Nuclear extracts (input) and immunoprecipitated fractions (IP) were subjected to Western blot analysis using specific antibodies against Sin3B, HDAC2, Tip60 and MRG proteins. Western blot analysis showed the association of RBP2 with the MRG15-containing HDAC complex. (E, F) Immunofluorescence images of HeLa cells expressing FLAG-tagged RBP2 (F-RBP2). Cells were fixed with cold methanol, followed by immunostaining with anti-FLAG M2 antibody for F-RBP2 (left), an anti-MRG15 antibody (middle of E) or an anti-RNA polymerase II antibody (H5, middle of F). Merged images of green (F-RBP2) and magenta (MRG15 or H5) staining are shown on the right.

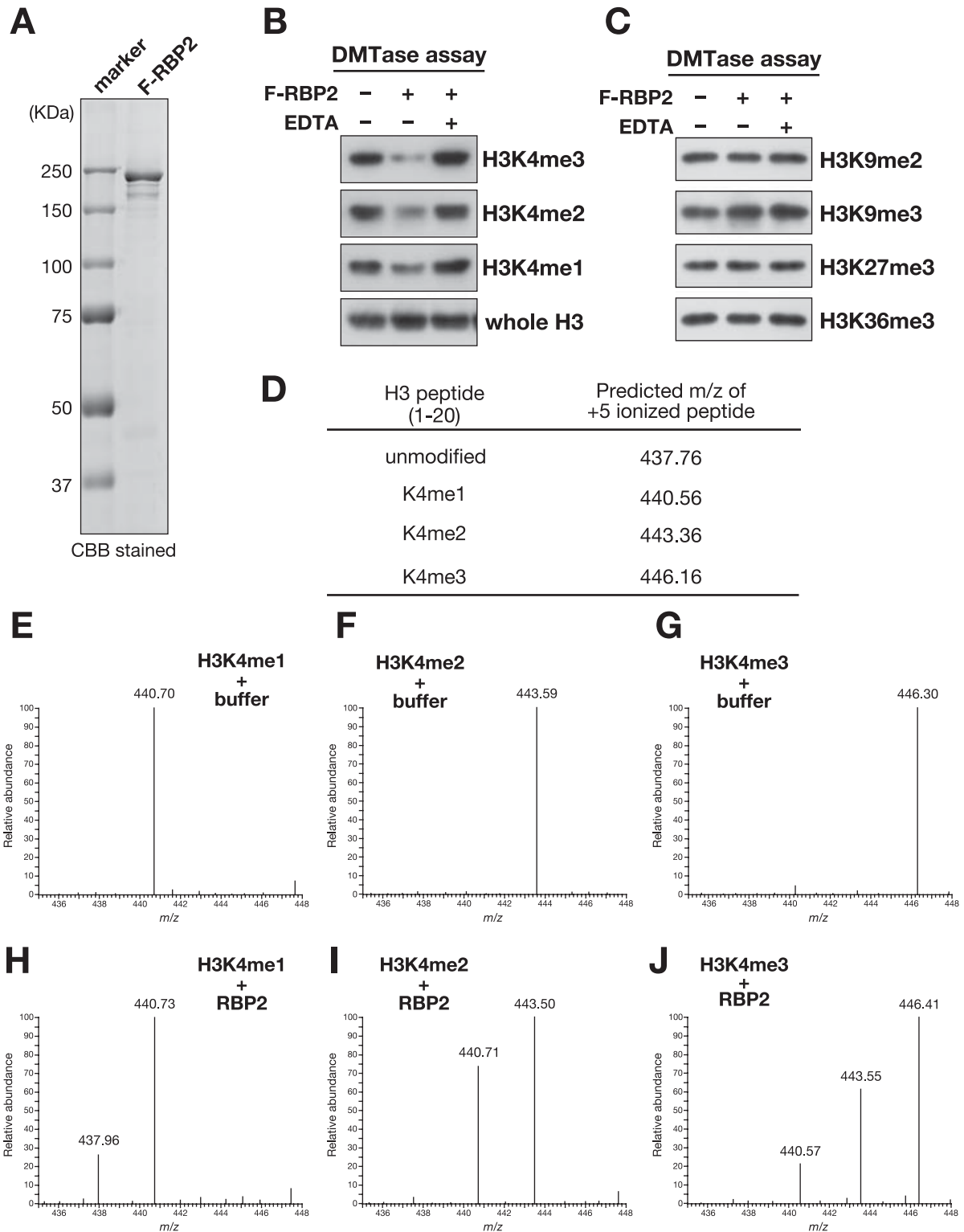
Figure 4 Over-expression of full-length RBP2 results in decreased H3K4 methylation in HeLa cells. (A) Full-length RBP2 was transiently expressed in HeLa cells as a FLAG fusion protein. Cells were fixed with cold methanol followed by indirect immunofluorescence staining using antibodies against H3K4me3, H3K9me3, H3K36me2 or H3K36me3 (left column) and an anti-FLAG antibody to detect RBP2 (middle column). Merged images of the green (modified histone H3) and magenta (RBP2) staining are shown in the right column. Representative cells expressing RBP2 are marked with white arrows. (B) Wild-type (top) or mutant (H483A, bottom) RBP2 was transiently expressed in HeLa cells as a FLAG-fusion protein. Cells were fixed with cold methanol followed by indirect immunofluorescence staining using antibodies against H3K4me3, H3K4me2 or H3K4me1 (left column) and an anti-FLAG antibody to visualize the wild-type or mutant RBP2 (middle column). Merged images are shown in the right column as in (A).



complexes, as previously demonstrated for Eaf3 in *S. cerevisiae* (Carrozza *et al.* 2005; Joshi & Struhl 2005; Keogh *et al.* 2005). Viewed in a different light, the lower H3K4me levels in transcribed regions might also correlate with the function of the RBP2, as it is physically associated with the MRG15-containing HDAC complexes. To test this hypothesis, we investigated the effect of over-expressing RBP2 on the H3K4 methylation levels by immunostaining. Over-expression of F-RBP2 greatly reduced the overall H3K4me1, H3K4me2 and H3K4me3 levels in HeLa cells (Fig. 4A,B, indicated by white arrows). This effect appeared to be specific to H3K4 methylation, because no detectable change was observed on the levels of H3K9me3, H3K36me3 or H3K27me3 (Fig. 4A). To investigate whether or not these RBP2-mediated effects were direct, we introduced a single amino acid substitution, H483A, into the RBP2 JmjC domain (RBP2^{H483A}). Analogous mutation of corresponding histidines was reported to abolish the demethylase activity of JHDM1 and JHDM2A both *in vivo* and *in vitro* (Tsukada *et al.* 2006; Yamane *et al.* 2006). As shown in Fig. 4B, the over-expression of RBP2^{H483A} did not alter the overall cellular levels of mono-, di- or tri-methyl-H3K4. These results suggest that RBP2 is an H3K4-specific demethylase that potentially reverses all

three methylation states of H3K4 and that the conserved JmjC domain is responsible for the demethylase activities.

We wished to assess the H3K4me demethylase activity of RBP2 directly *in vitro*. Recombinant, baculovirus-expressed F-RBP2 (Fig. 5A) was incubated with free histones prepared from HeLa cells (Fig. 5B,C). F-RBP2 reduced the level of H3K4me3, H3K4me2 and H3K4me1 of bulk histones (Fig. 5B), but did not change the level of H3K9me2, H3K9me3, H3K27me3 or H3K36me3 (Fig. 5C). Addition of EDTA abolished demethylase activity of RBP2 in common with that of other JmjC-domain histone demethylases. We further verified its enzymatic activity using a K4-methylated H3 peptides and LC-MS. Either K4-mono-, di- or tri-methylated histone H3 peptide was incubated with RBP2 and subjected to LC-MS analysis. By analyzing representative + 5 ion-charged peptides (Fig. 5D), we found that recombinant RBP2 efficiently reversed methyl groups from all three K4-methylated H3 peptides (Fig. 5E–J) (mass of 2.8 Da corresponded to 14 Da difference of original peptide). We also confirmed that both Fe(II) and α -ketoglutaric acid were required for RBP2's enzymatic activity (Supplementary Fig. S2). Taken together, these data, from experiments *in vivo* and *in vitro*, strongly argue that RBP2 is a histone H3K4me-specific demethylase.



RBP2 affects H3K4 trimethylation in transcribed regions

RBP2 was initially identified as an RB binding protein by yeast two-hybrid screening, and subsequent studies primarily focused on its role at promoter regions to regulate transcriptional activity (Kim *et al.* 1994; Chan & Hong 2001; Benevolenskaya *et al.* 2005). While it is most likely that a subpopulation of RBP2 molecules participates in transcriptional regulation via targeting upstream promoter regions, its physical interaction with MRG15-containing HDAC complexes also implies that it controls H3K4 methylation levels within transcribed regions. To test this idea, we knocked down RBP2 in HeLa cells by RNAi and analyzed the histone methylation states at representative active gene loci (*RPL13a* and *GAPDH*) (Fig. 6). We conducted chromatin immunoprecipitation (ChIP) analysis using antibodies against K4- or K36-methylated histone H3 (H3K4me3, H3K4me2, H3K4me1 and H3K36me3), K4-unmodified H3, whole H3, RBP2 and MRG15, followed by quantitative PCR analysis. Quantified enrichments of precipitated DNA (Supplementary Figs S3 and S4) were normalized using levels of whole H3 (Fig. 6D,E). In control experiments, ChIP detected H3K4me3 and H3K4me2 at *RPL13a* and *GAPDH* loci; these were present in the promoter region, peaked in exon3, and gradually decreased towards the distal transcribed region (Fig. 6D,E, blue bars). In contrast, H3K36me3 was not detected in the promoter regions but was present across transcribed regions. Both RBP2 and MRG15 were detected apparently uniformly throughout these active genes (Fig. 6D,E and Supplementary Fig. S3).

When we transfected siRNAs targeting RBP2 transcripts, endogenous RBP2 levels were efficiently

reduced as confirmed by Western blotting (Fig. 6A). Chromatin-bound RBP2 also decreased, to 29%–78% of original levels (Fig. 6D,E, RBP2, red bars). Knockdown of RBP2 led to a marked increase in the levels of H3K4me3 and H3K4me2 at exon3 (P2, $P < 0.05$) and the distal transcribed regions of the *RPL13a* locus, while inducing a negligible change within the promoter region (Fig. 6D). These increases were consistent with proportional reductions of K4-unmodified H3 (Fig. 6D, H3K4-unmod.). Similarly increase in H3K4me3 was observed at exon3 (P2, $P < 0.05$) and the distal transcribed regions of the *GAPDH* locus (Fig. 6E). We also observed an increase in the level of H3K4me3 and a slight reduction of H3K4me1 at promoter region (P1) of the *GAPDH* locus, although significance of these changes was not clear (P1, $P > 0.05$). No obvious increase of H3K4me2 was detected throughout the transcribed regions of the *GAPDH* locus (Fig. 6E). The levels of H3K36me3 did not change significantly following RBP2 knockdown (Fig. 6D,E). Taken together, these results support the idea that RBP2 regulates the level of H3K4 methylation within the transcribed regions of active genes.

In *S. cerevisiae*, H3K36 methylation is considered to function upstream of deacetylation events (Carrozza *et al.* 2005; Joshi & Struhl 2005; Keogh *et al.* 2005). Based on this it is therefore possible that RBP2 is recruited to the transcribed regions through interactions involving the MRG15 complexes. To investigate this, we knocked down the endogenous HeLa cell MRG15 by RNAi (Fig. 6A) and analyzed this effect on the levels of H3K4- and H3K36-methylation and H3K9/K14-acetylation at *RPL13a* locus (Fig. 7A and Supplementary Fig. S4). Although we did not detect any significant changes in levels of H3K4me3, H3K4me1 or H3K4me36 ($P > 0.05$), we were able to observe reduced levels of RBP2 and increased levels of H3K4me2 at the *RPL13a* transcribed regions following MRG15 knockdown (Fig. 7A, P2; $P < 0.05$). In contrast to the deletion phenotype of *S. cerevisiae* Eaf3, the levels of H3K9/K14-acetylation at the *RPL13a* transcribed regions were not clearly changed following MRG15 knockdown (Supplementary Fig. S4B). Taken together, these results indicate that RBP2 is recruited to the transcribed regions, at least partly, by interacting with the MRG15-containing complex, which results in the down-regulation of H3K4 methylation at these transcribed regions. The partial effect of MRG15 knockdown might be attributable to the fact that RBP2 recruitment was controlled by additional interactions with other unidentified components, or that, in the MRG15-deleted cells, MRGX may play the part of MRG15 in recruiting RBP2 to the transcribed regions.

Figure 5 RBP2 is a histone H3K4-specific demethylase. (A) Coomassie-stained SDS-PAGE gel of the purified FLAG-tagged RBP2 (F-RBP2) expressed in Sf9 cells. (B, C) Histone demethylase (DMTase) activity of recombinant F-RBP2. HeLa cell core histones were incubated in the presence (+) or absence (–) of F-RBP2 and EDTA (a divalent cation chelator). Following the demethylation reaction, the histone methylation levels were analyzed by Western blotting with modification-specific or whole histone H3 antibodies. (D) Summary of predicted m/z of +5 ionized histone H3 peptide (ARTKQTARKSTGGKAPRKQR). Mass of 2.8 Da corresponds to 14 Da difference of original peptide. (E–J) Mass spectrometry analysis of demethylation of H3K4me1, H3K4me2 and H3K4me3 peptides by purified F-RBP2. Number represents the mass of the substrate and converted peptides. Representative +5 ion-charged peptides are shown.

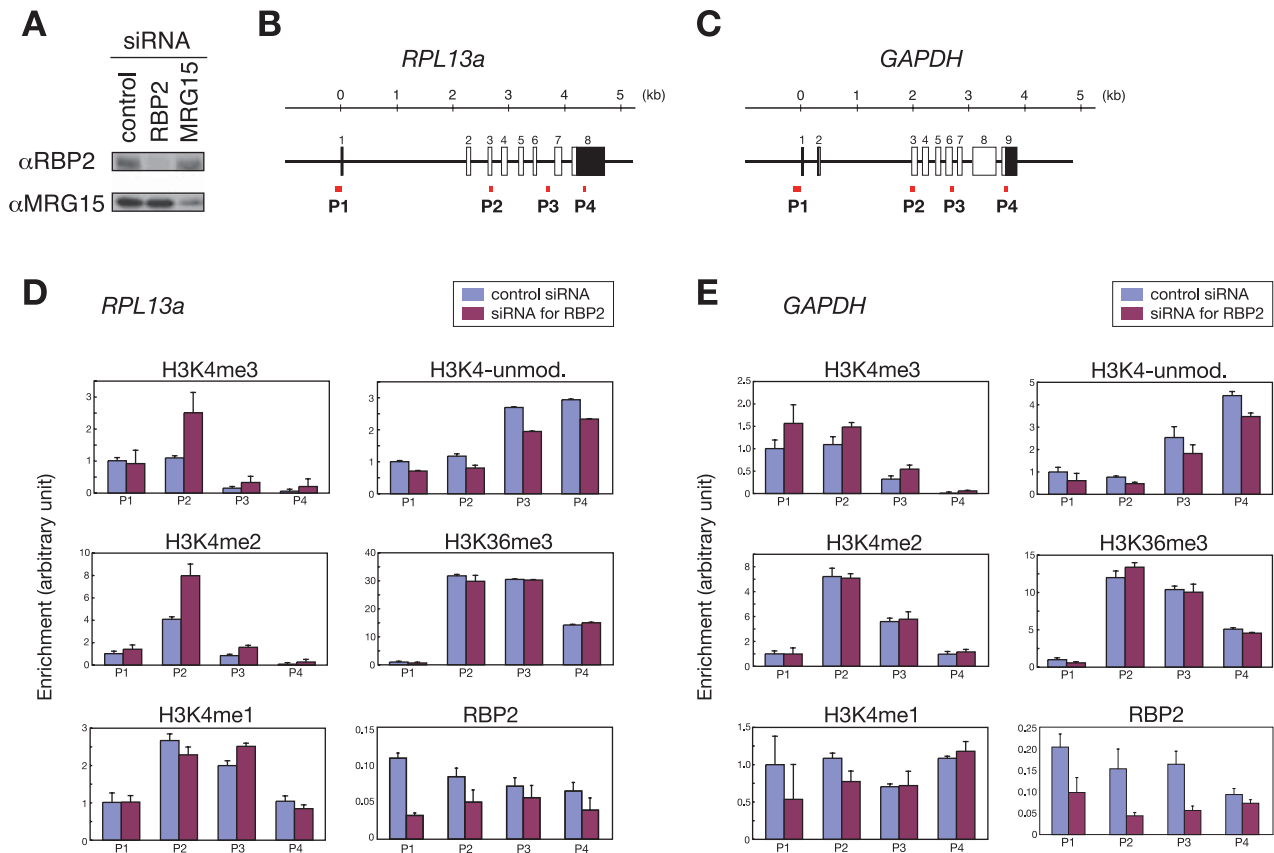


Figure 6 RBP2 knockdown results in increased H3K4 methylation at transcribed regions. (A) Knockdown of RBP2 in HeLa cells by siRNA. HeLa cells were transfected with control or RBP2 siRNA, and 24 h later the endogenous RBP2 or MRG15 was analyzed by Western blotting using polyclonal antibodies. (B, C) Schematic diagrams of the *RPL13a* (B) and *GAPDH* (C) gene loci. Exons are indicated by numbered boxes and black and white areas indicate UTRs and ORFs, respectively. The PCR-amplified regions (P1–P4) in the ChIP analysis are indicated with red bars. (D, E) Results of chromatin immunoprecipitation (ChIP) experiments monitoring the distribution of H3K4 tri-, di- and monomethylation, unmodified H3K4, H3K36 trimethylation and RBP2 at the *RPL13a* (D) and *GAPDH* (E) loci in control knockdown (blue) or RBP2 knockdown (red) HeLa cells. The degree of enrichment achieved in the ChIP was analyzed by real-time PCR. The enrichment ratio for modified or unmodified histone H3 (% input, Supplementary Fig. S3) were normalized using the levels of whole H3 and means of the relative ratio against the value of P1 region in control knockdown experiments are plotted on the y -axis (arbitrary unit). The value for RBP2 is the original ratio of precipitated DNA to input DNA (%). The position of the amplified regions of each locus is indicated on the x -axis. Error bars represent \pm SD of three independent replicates.

Discussion

We here report a biochemical and cellular characterization of MRG15 family proteins that reveals a novel interaction between the MRG15 complex and a JmjC domain protein, RBP2. We further demonstrated that RBP2 plays a critical role in histone H3K4 demethylation and functions in maintaining a lower H3K4 methylation state across transcribed regions. Our findings provide new evidence that MRG15-containing complexes are key modulator of H3K4 methylation in transcribed regions.

Co-localization of MRG15 and hyperphosphorylated RNA polymerase II

Our data demonstrate that MRG15 predominantly localizes to the nucleus, and its apparent distribution pattern is altered by different fixation conditions (Fig. 1A). These observations clearly concur with those previously reported for Ser²-hyperphosphorylated RNA polymerase II (Guillot *et al.* 2004) and we extend them by showing that the MRG15 signals co-localize with those of RNA polymerase II. Since methanol is a relatively poor structural fixative, there are issues regarding the biological

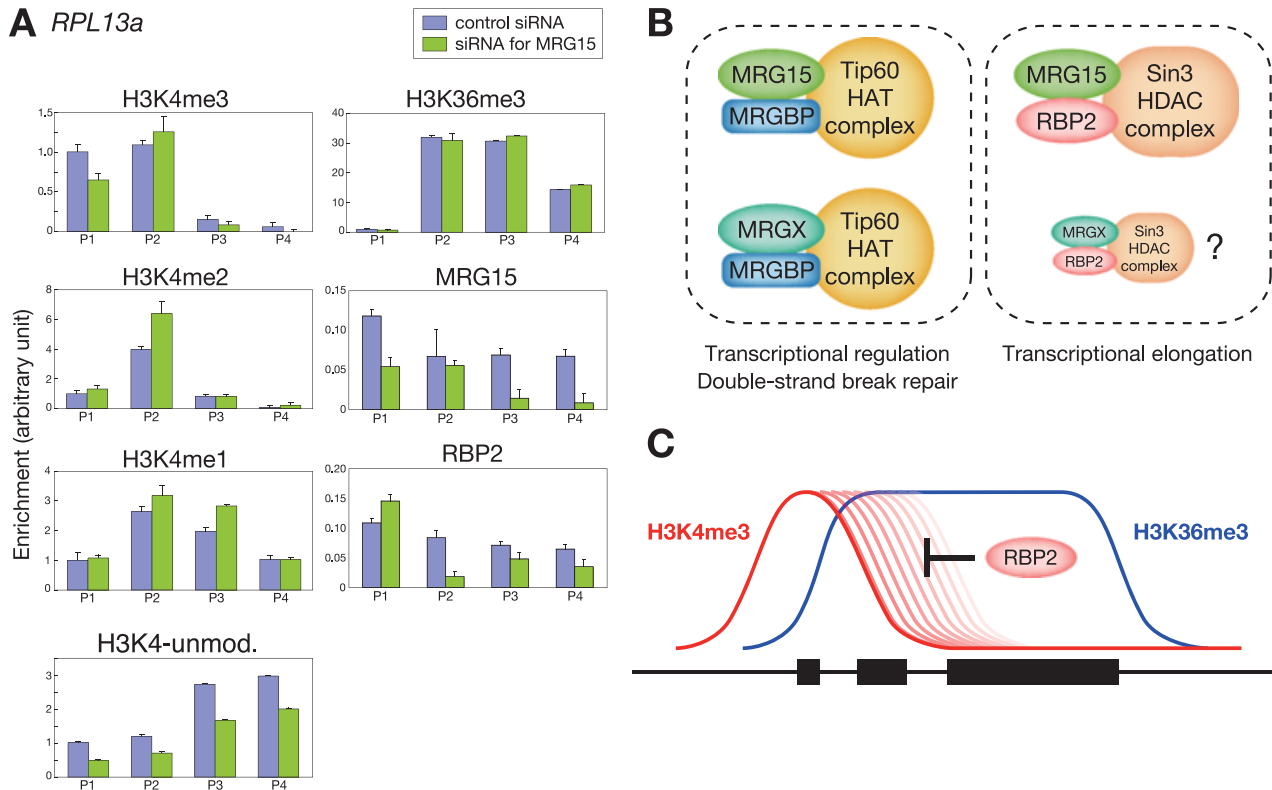


Figure 7 MRG15 is required for RBP2-induced H3K4 demethylation. (A) Results of ChIP experiment monitoring the distribution of H3K4 tri-, di- and monomethylation, unmodified H3K4, H3K36 trimethylation, RBP2 and MRG15 at the *RPL13a* loci in control (blue) or MRG15 knockdown (green) HeLa cells. The degree of enrichment achieved in the ChIP was analyzed by real-time PCR. The enrichment ratios for modified or unmodified histone H3 (% input, Supplementary Fig. S4) were normalized using levels of whole H3 and means of the relative ratio against the value of P1 in control knockdown experiments are plotted on the y -axis (arbitrary unit). The value for RBP2 and MRG15 indicates the original ratio of precipitated DNA to input DNA (%). The position of the amplified regions of each locus is indicated on the x -axis. Error bars represent \pm SD of three independent replicates. (B) Schematic representation of the MRG protein complexes. Both MRG15 and MRGX are stable components of distinct HAT and HDAC complexes, while MRGBP is specifically associated with the Tip60 HAT complex. RBP2 interacts with the MRG15/MRGX-containing HDAC complexes, showing higher affinity for the MRG15-containing complex. (C) Model for RBP2 function in transcriptional regulation. The transcriptional initiation sites and distal transcribed regions are differentially marked by histone H3K4 and H3K36 methylation. The demethylation activity of RBP2 facilitates the maintenance of lower H3K4 methylation at coding regions, which may ensure the transcriptional elongation steps.

relevance of the “speckle”-like distribution of RNA polymerase II. However, our observations revealed clear co-localization of RNA polymerase II with MRG15, suggesting that these focal RNA polymerase II-enriched distributions represent specific nuclear subdomains engaged in transcriptional elongation. This interpretation is also consistent with studies on *S. cerevisiae* Eaf3 in the Rpd3S complex and is further supported by delocalization of characteristic focal distributions in response to actinomycin D treatment, a widely used transcriptional inhibitor (Supplementary Fig. S1C). Based on our findings that MRG15 and MRGX are components of distinct HAT

and HDAC complexes, we favor the view that the nucleoplasmic distribution and focal accumulation of MRG15 represent discrete subpopulations of MRG15-containing complexes performing dedicated cellular functions.

MRG15 and MRGX form distinct multiprotein complexes

Immunoaffinity purification analyses revealed that MRG15 and MRGX each form distinct multiprotein complexes of superimposable protein composition (Fig. 2A). This

suggests that the MRG15 chromodomain is not essential for complex formation and that it functions in recruitment to specific chromosomal regions. Although *MrgX*-null mice lack a phenotype, the overlapping and complementary functions of Mrg15 and MrgX are suggested by the early lethality of double knockout embryos (Tominaga *et al.* 2005b). It is therefore likely that MRGX is able to partially rescue the function of MRG15 by recruiting similar protein complexes to the target chromatin during early embryogenesis. In this study, we demonstrated that like MRG15, MRGX is also associated with both HAT- and HDAC-complexes. The mechanisms that partition MRG15 and MRGX between their respective complexes and determine their relative abundances, however, remain unknown. Functional differences between MRG15 and MRGX are implied from the presence of a chromodomain in the former, but it is also possible that the respective balance of their association with the HAT- and HDAC-complexes is also different (Figs 3 and 7B). Our observation that MRGBP expression led to an increase in endogenous levels of MRG15 and MRGX could be relevant to this issue (Fig. 2B). Although the specific function of MRGBP in HAT complexes has yet to be characterized, it is likely that it plays a key role in controlling the levels of MRG15 and MRGX associated with the Tip60-HAT complexes (Fig. 7B).

Newly identified factors associated with the MRG15-containing complex

Affinity purification of the MRG15-containing complexes revealed six subunits not previously described in this context: ZNF131, mbt domain containing 1 (MBTD1), three hnRNPs and RBP2. ZNF131 is a typical BTB/POZ (broad-complex, tramtrack and bric-a-brac/poxvirus and zinc finger) domain and multiple zinc fingers in its C-terminal half (Trappe *et al.* 2002). Although the precise function of ZNF131 has yet to be identified, studies on other family members suggest roles in transcriptional repression in which the zinc-finger domain binds the promoter of genes involved in cellular proliferation and differentiation (Collins *et al.* 2001). MBTD1 contains four malignant brain tumor (MBT) domains originally identified in the *Drosophila lethal(3)malignant brain tumor* gene product (Wisnar *et al.* 1995). The MBT domain is structurally similar to the chromodomain and binds H3K4me1, H4K20me1 and H4K20me2 (Maurer-Stroh *et al.* 2003; Kim *et al.* 2006). Although it is an open question whether the MBT domains in MBTD1 have kinetics for specific methyl histones analogous to other MBT domain-containing proteins, it is tempting to speculate that it binds H3K4me1 to facilitate MRG15-

containing complex targeting to specific chromosomal regions. Any clues to functional links between MRG15 and the three hnRNPs are elusive at this time.

RBP2 down-regulates the H3K4 methylation at transcribed regions

RBP2 was originally identified as a RB binding protein. Several functional analyses demonstrate a repressive role for RBP2 in RB-mediated transcriptional activation, but it, paradoxically, cooperates with RB to activate several homeotic genes (Benevolenskaya *et al.* 2005). RBP2 also physically associates with several nuclear hormone receptors to enhance gene expression (Chan & Hong 2001). Although these studies highlight the importance of RBP2 in transcriptional activation and repression via its action at promoter regions, its functional contribution for transcribed regions has yet to be addressed. In this study, we provide evidence that RBP2 interacts with MRG15-containing HDAC complexes and that it down-regulates H3K4 methylation across transcribed regions (Figs 6 and 7B,C).

Although we demonstrate the effect of RBP2 knockdown to increase H3K4me3 and H3K4me2 at the *RPL13a* and *GAPDH* transcribed regions, it is unclear how the lower H3K4 methylation states contribute to repress aberrant intragenic transcription in HeLa cells. We did not detect aberrant *RPL13a* or *GAPDH* transcripts following RBP2 or MRG15 knockdown (data not shown), implying the existence of other cooperative or alternative mechanisms, such as hypoacetylation states, might act to suppress aberrant transcriptional initiation from intragenic regions in HeLa cells. In our ChIP experiments, RBP2 was also detected at the upstream promoter regions and its association level decreased following RBP2 knockdown. However, the levels of H3K4me3 and H3K4me2 were not changed at the *RPL13a* promoter regions (Fig. 6D). Although a slight increase of H3K4me3 and a reduction of H3K4me1 were observed at the *GAPDH* promoter region (Fig. 6E), significance of these changes is unclear ($P > 0.05$). It is possible that RBP2's activity is differentially regulated at the promoter and distal transcribed regions, which may be accompanied by the changes in interacting partner proteins. Another possibility is that other JARID1 family proteins play a redundant role specifically at the promoter regions. We also found there were substantial pre-existing H3K4me3 within the transcribed regions. The biological significance of pre-existing H3K4me3 remains unclear, although it is possible that the level of H3K4me3 in transcribed regions correlates with the expression level or promoter activity of the corresponding genes; a relatively strong promoter activity of *GAPDH*, for example, might

seed a high level of H3K4me3 from the initiation site to the rest of the transcriptional unit in a manner that is reversed by RBP2.

In the present study, we focused on RBP2 function in general transcriptional regulation, based on precedents provided by Eaf3- and Rpd3S-containing complexes in *S. cerevisiae*. It is likely that RBP2 is recruited to specific promoter regions either independently of, or in conjunction with, MRG15-containing HDAC complexes, to regulate expression of target genes. Transcriptional repression by RB (which binds RBP2) of E2F target genes such as *cyclin E* is closely linked with the recruitment of HDAC complexes and the histone H3K9 methyltransferase, SUV39H (Frolov & Dyson 2004). RBP2 might therefore play a role in the RB-mediated dynamic regulation of cell-cycle responsive genes. Several lines of evidence support a role for Tip60-associating MRG family proteins in DNA double strand break (DSB) repair (Kusch *et al.* 2004). Although we showed that RBP2 is associated with MRG15-containing HDAC complex, it is possible that RBP2 is also involved with the DSB repair process. In analysis of RBP2-associating proteins, we demonstrated that MRG15 and HDAC-associated proteins were stably associated with RBP2 (Fig. 3C). Interestingly, we also identified several novel proteins, which were implicated in DSB repair (our unpublished observation). The possible role of RBP2 in DSB repair could be tested by a detailed analysis using an appropriate experimental system.

Experimental procedures

Cell culture and antibodies

T-Rex HeLa cells (Invitrogen) were cultured in EMEM (Cambrex) with 1 mM glutamic acid or in EMEM (Nakalai tesque) supplemented with 1 mM sodium pyruvate (GIBCO). HeLa cells (CCL2) and HEK293T cells were cultured in DMEM (Sigma). All culture medium were supplemented with 10% fetal calf serum (Equitech-Bio). Stable T-Rex HeLa cell lines expressing FLAG-MRG15, FLAG-MRGX, FLAG-MRGBP or FLAG-RBP2 under tetracycline induction were isolated and maintained in medium containing 100 µg/mL zeocin (Invitrogen). Antibodies used in this study were: anti-H3K4me3 (ab8580, Abcam; monoclonal 16H10), anti-H3K4me2 (07-030, Upstate; monoclonal 27A6), anti-H3K4me1 (ab8895, Abcam), anti-K3K4-unmodified (monoclonal 13C12), anti-H3K9me3 (ab8898, Abcam), anti-H3K9me2 (07-212, Upstate), anti-H3K27me3 (07-449, Upstate), anti-H3K36me3 (ab9050, Abcam), anti-H3K36me2 (ab9049, Abcam) and anti-histone H3 (ab1791, Abcam), anti-Ser²-phosphorylated RNA polymerase II (H5, Covance). All monoclonal antibodies for specific histone tails were kindly gifted from H. Kimura and N. Nozaki. Anti-MRG15 and anti-MRGX rabbit polyclonal antibodies were raised against each

of 6His-tagged full-length recombinant protein and affinity-purified using columns cross-linked with GST-MRG15 (aa 1–88) and GST-MRGX (aa 1–72), respectively. Anti-MRGBP rabbit polyclonal antibody was raised against and affinity-purified using full-length recombinant protein. Anti-RBP2 rabbit polyclonal antibodies were raised against and affinity-purified using a GST-fused C-terminal RBP2 fragment (aa 1622–1690).

Plasmids

The open reading frames (ORFs) of human MRG15 (NM_006791), MRGX (NM_012286), MRGBP (NM_018270) and RBP2 (NM_001042603) were cloned by RT-PCR using mRNAs isolated from HeLa cells as a PCR template. Total RNA was isolated using TRIzol (Invitrogen) according to the manufacturer's instructions. Complementary DNAs (cDNAs) were synthesized using SuperScript III (Invitrogen) with oligo dT primer, and the corresponding cDNAs were amplified using the Expand High Fidelity PCR system (Roche) with specific sets of primers. The PCR products were cloned into the pCRII vector using the TOPO-TA cloning Kit (Invitrogen) or pBlueScript (Stratagene), sequenced, and then subcloned into expression plasmids. To obtain Tet-inducible expression plasmids, FLAG-fused ORF was introduced into the pCDNA4/TO vector (Invitrogen).

Affinity purification of MRG15 complex

Forty milligrams of nuclear extract prepared from T-Rex HeLa cell lines (Invitrogen) expressing FLAG-tagged MRG15, MRGX, MRGBP or RBP2 was diluted to 2 mg/mL with 0.3 K-IP buffer (50 mM HEPES [pH 7.9], 0.3 M KCl, 10% glycerol, 0.2 mM EDTA, 0.5 mM PMSE, 0.1% Triton X-100). The diluted extracts were pre-cleared with Sepharose CL-4B (GE Healthcare) for 1 h at 4 °C, and then incubated with anti-FLAG-M2 agarose (Sigma) for 8 h at 4 °C with gentle rotation. The resin was washed sequentially with 2 column volumes of 0.25 K-IP buffer, 1 column volume of 0.3 K-IP buffer and 1 column volume of 0.25 K-IP buffer. Bound proteins were eluted twice with 0.3 K-IP buffer containing 0.25 mg/mL 3× FLAG peptide for 4 h at 4 °C with rotation. The eluates were precipitated with a 2-times volume of ethanol, resolved on a 4%–20% gradient SDS-PAGE gel (Daiichi) and stained using SilverQuest (Invitrogen). Each specific polypeptide band was excised, destained and trypsinized for LC-MS/MS analysis.

Indirect immunofluorescence

Cells were fixed with –80 °C pre-cooled methanol or 3.7% methanol-free formaldehyde (Polyscience) in culture medium for 20–30 min at room temperature. After several washes with PBS, the formaldehyde-fixed cells were permeabilized with 0.2% Triton X-100 in PBS. Fixed cells were blocked by treatment with 1% bovine serum albumin in PBS at room temperature for 1 h followed by incubation with primary antibody for 3 h at room temperature. After being washed with PBS, the cells were stained with Alexa488-conjugated or Alexa546-conjugated fluorescent

secondary antibodies for 3 h at room temperature. After being washed with PBS, the cells were mounted in 90% glycerol. Fluorescence microscopic images were obtained on a CoolSNAP HQ (Photometrics) and IX71 (Olympus) based three-dimensional microscope system. Three-dimensional optical section images were taken at 0.5 μm focus intervals using METAMORPH (Universal Imaging), and the acquired images were de-convolved and analyzed by SOFTWORX (Applied Precision).

Histone demethylase assay

FLAG-tagged RBP2 (F-RBP2) was expressed in Sf9 cells using the Bac-to-Bac Baculovirus Expression System (Invitrogen) and purified with anti-FLAG M2 agarose (Sigma) followed by elution with 3X FLAG peptide (Sigma). Eluted F-RBP2 protein was dialyzed against D-buffer (25 mM HEPES-KOH [pH7.5], 50 mM KCl, 10% glycerol, 1 mM DTT, 0.2 mM PMSF) and concentrated using a Microcon YM-30 (Amicon). Five micrograms of free histones prepared from HeLa cells or synthesized histone H3 peptides were incubated with 1–2 μg of F-RBP2 in 50 μL of DMT assay buffer (50 mM HEPES-KOH [pH7.5], 50 mM KCl, 75 μM $\text{Fe}(\text{NH}_4)_2(\text{SO}_4)_2 \cdot 6\text{H}_2\text{O}$, 1 mM α -ketoglutaric acid, 1 mM PMSF) for 2 h at 37 °C. The reaction was terminated by adding 2 mM EDTA. Histones were subjected to SDS-PAGE and analyzed by immunoblotting using specific antibodies. K4-methylated peptides were analyzed by LC-MS analysis (Thermo Electron, Finnigan LTQ).

Chromatin Immunoprecipitation (ChIP)

ChIP was carried out basically according to the instructions of the ChIP Assay Kit (Upstate). All buffers used in the ChIP assay were supplemented with protease inhibitor cocktail (Complete, Roche). Briefly, siRNA-transfected HeLa cells were fixed with 1% formaldehyde for 10–15 min at 37 °C. The cell suspension in SDS lysis buffer (50 mM Tris, pH 8.0, 1% SDS, 10 mM EDTA) was sonicated with a Branson Sonifer 250 (level 1.2, constant 12 s by 6 times). The sonicated samples were diluted with ChIP dilution buffer (16.7 mM Tris, pH 8.0, 167 mM NaCl, 0.01% SDS, 1.1% Triton X-100, 1.2 mM EDTA) and immunoprecipitated with specific antibodies at 4 °C overnight. Protein A-agarose pre-equilibrated with TE buffer containing 200 $\mu\text{g}/\text{mL}$ salmon sperm DNA and 0.5 mg/mL BSA was added and then washed sequentially with low-salt buffer (20 mM Tris-HCl [pH 8.0], 150 mM NaCl, 0.1% SDS, 1% Triton X-100, 2 mM EDTA), high-salt buffer (20 mM Tris-HCl [pH 8.0], 500 mM NaCl, 0.1% SDS, 1% Triton X-100, 2 mM EDTA), LiCl buffer (10 mM Tris-HCl [pH 8.0], 0.25 M LiCl, 1% NP40, 1% sodium deoxycholate, 1 mM EDTA) and TE buffer. The protein-DNA complexes were de-crosslinked overnight at 65 °C, and finally, the immunoprecipitated DNA was recovered by phenol/chloroform extraction and ethanol precipitation after Poteinase K treatment. ChIPed DNA was analyzed by an ABI 7300 real-time PCR system (Applied Biosystems). For sample amplification, qPCR Mastermix Plus (Eurogentec) was used. The primers used in real-time PCR are listed in Supplementary Table S1.

Acknowledgements

We thank H. Kimura and N. Nozaki for monoclonal antibodies, and M. Okano, T. Perry and M. Royle for critical reading of and comments on this manuscript. We also thank our laboratory members in Riken, CDB and S. Seno for the excellent secretarial work. None of authors have a financial interest related to this work. This research was supported by Grants-in-Aid from the Ministry of Education, Culture, Sports, Science and Technology of Japan.

References

- Benevolenskaya, E.V., Murray, H.L., Branton, P., Young, R.A. & Kaelin, W.G., Jr. (2005) Binding of pRB to the PHD protein RBP2 promotes cellular differentiation. *Mol. Cell* **18**, 623–635.
- Bertram, M.J., Berube, N.G., Hang-Swanson, X., Ran, Q., Leung, J.K., Bryce, S., Spurgers, K., Bick, R.J., Baldini, A., Ning, Y., Clark, L.J., Parkinson, E.K., Barrett, J.C., Smith, J.R. & Pereira-Smith, O.M. (1999) Identification of a gene that reverses the immortal phenotype of a subset of cells and is a member of a novel family of transcription factor-like genes. *Mol. Cell. Biol.* **19**, 1479–1485.
- Bertram, M.J. & Pereira-Smith, O.M. (2001) Conservation of the MORF4 related gene family: identification of a new chromo domain subfamily and novel protein motif. *Gene* **266**, 111–121.
- Bregman, D.B., Du, L., van der Zee, S. & Warren, S.L. (1995) Transcription-dependent redistribution of the large subunit of RNA polymerase II to discrete nuclear domains. *J. Cell Biol.* **129**, 287–298.
- Cai, Y., Jin, J., Tomomori-Sato, C., Sato, S., Sorokina, I., Parmely, T.J., Conaway, R.C. & Conaway, J.W. (2003) Identification of new subunits of the multiprotein mammalian TRRAP/TIP60-containing histone acetyltransferase complex. *J. Biol. Chem.* **278**, 42733–42736.
- Carrozza, M.J., Li, B., Florens, L., Suganuma, T., Swanson, S.K., Lee, K. K., Shia, W.J., Anderson, S., Yates, J., Washburn, M.P. & Workman, J.L. (2005) Histone H3 methylation by Set2 directs deacetylation of coding regions by Rpd3S to suppress spurious intragenic transcription. *Cell* **123**, 581–592.
- Chan, S.W. & Hong, W. (2001) Retinoblastoma-binding protein 2 (Rbp2) potentiates nuclear hormone receptor-mediated transcription. *J. Biol. Chem.* **276**, 28402–28412.
- Collins, T., Stone, J.R. & Williams, A.J. (2001) All in the family: the BTB/POZ, KRAB, and SCAN domains. *Mol. Cell. Biol.* **21**, 3609–3615.
- Doyon, Y. & Cote, J. (2004) The highly conserved and multi-functional NuA4 HAT complex. *Curr. Opin. Genet. Dev.* **14**, 147–154.
- Doyon, Y., Selleck, W., Lane, W.S., Tan, S. & Cote, J. (2004) Structural and functional conservation of the NuA4 histone acetyltransferase complex from yeast to humans. *Mol. Cell. Biol.* **24**, 1884–1896.
- Eisen, A., Utley, R.T., Nourani, A., Allard, S., Schmidt, P., Lane, W.S., Lucchesi, J.C. & Cote, J. (2001) The yeast NuA4 and *Drosophila* MSL complexes contain homologous subunits important for transcription regulation. *J. Biol. Chem.* **276**, 3484–3491.

- Frolov, M.V. & Dyson, N.J. (2004) Molecular mechanisms of E2F-dependent activation and pRB-mediated repression. *J. Cell Sci.* **117**, 2173–2181.
- Gavin, A.C., Bosche, M., Krause, R., *et al.* (2002). Functional organization of the yeast proteome by systematic analysis of protein complexes. *Nature* **415**, 141–147.
- Guillot, P.V., Xie, S.Q., Hollinshead, M. & Pombo, A. (2004) Fixation-induced redistribution of hyperphosphorylated RNA polymerase II in the nucleus of human cells. *Exp. Cell Res.* **295**, 460–468.
- Hampsey, M. & Reinberg, D. (2003) Tails of intrigue: phosphorylation of RNA polymerase II mediates histone methylation. *Cell* **113**, 429–432.
- Joshi, A.A. & Struhl, K. (2005) Eaf3 chromodomain interaction with methylated H3-K36 links histone deacetylation to Pol II elongation. *Mol. Cell* **20**, 971–978.
- Kaplan, C.D., Laprade, L., and Winston, F. (2003) Transcription elongation factors repress transcription initiation from cryptic sites. *Science* **301**, 1096–1099.
- Keogh, M.C., Kurdistani, S.K., Morris, S.A., *et al.* (2005) Cotranscriptional set2 methylation of histone H3 lysine 36 recruits a repressive Rpd3 complex. *Cell* **123**, 593–605.
- Kim, J., Daniel, J., Espejo, A., Lake, A., Krishna, M., Xia, L., Zhang, Y. & Bedford, M.T. (2006). Tudor, MBT and chromo domains gauge the degree of lysine methylation. *EMBO Rep.* **7**, 397–403.
- Kim, Y.W., Otterson, G.A., Kratzke, R.A., Coxon, A.B. & Kaye, F.J. (1994) Differential specificity for binding of retinoblastoma binding protein 2 to RB, p107, and TATA-binding protein. *Mol. Cell. Biol.* **14**, 7256–7264.
- Klose, R.J., Kallin, E.M. & Zhang, Y. (2006) JmjC-domain-containing proteins and histone demethylation. *Nat. Rev. Genet.* **7**, 715–727.
- Krogan, N. J., Baetz, K., Keogh, M. C., Datta, N., Sawa, C., Kwok, T. C., Thompson, N. J., Davey, M. G., Pootoolal, J., Hughes, T. R., Emili, A., Buratowski, S., Hieter, P. & Greenblatt, J.F. (2004) Regulation of chromosome stability by the histone H2A variant Htz1, the Swr1 chromatin remodeling complex, and the histone acetyltransferase NuA4. *Proc. Natl. Acad. Sci. USA* **101**, 13513–13518.
- Kusch, T., Florens, L., Macdonald, W.H., Swanson, S.K., Glaser, R.L., Yates, J.R., 3rd, Abmayr, S.M., Washburn, M.P. & Workman, J. L. (2004) Acetylation by Tip60 is required for selective histone variant exchange at DNA lesions. *Science* **306**, 2084–2087.
- Lachner, M. & Jenuwein, T. (2002) The many faces of histone lysine methylation. *Curr. Opin. Cell Biol.* **14**, 286–298.
- Leung, J.K., Berube, N., Venable, S., Ahmed, S., Timchenko, N. & Pereira-Smith, O.M. (2001) MRG15 activates the B-myb promoter through formation of a nuclear complex with the retinoblastoma protein and the novel protein PAM14. *J. Biol. Chem.* **276**, 39171–39178.
- Maurer-Stroh, S., Dickens, N.J., Hughes-Davies, L., Kouzarides, T., Eisenhaber, F. & Ponting, C.P. (2003) The Tudor domain “Royal Family”: Tudor, plant Agenet, Chromo, PWWP and MBT domains. *Trends Biochem. Sci.* **28**, 69–74.
- Millar, C.B. & Grunstein, M. (2006) Genome-wide patterns of histone modifications in yeast. *Nat. Rev. Mol. Cell Biol.* **7**, 657–666.
- Nakayama, J., Xiao, G., Noma, K., Malikzay, A., Bjerling, P., Ekwall, K., Kobayashi, R. & Grewal, S.I. (2003) Alp13, an MRG family protein, is a component of fission yeast Clr6 histone deacetylase required for genomic integrity. *EMBO J.* **22**, 2776–2787.
- Reid, J.L., Moqtaderi, Z. & Struhl, K. (2004). Eaf3 regulates the global pattern of histone acetylation in *Saccharomyces cerevisiae*. *Mol. Cell. Biol.* **24**, 757–764.
- Shi, Y., Lan, F., Matson, C., Mulligan, P., Whetstine, J. R., Cole, P.A. & Casero, R.A. (2004) Histone demethylation mediated by the nuclear amine oxidase homolog LSD1. *Cell* **119**, 941–953.
- Strahl, B.D. & Allis, C.D. (2000) The language of covalent histone modifications. *Nature* **403**, 41–45.
- Tominaga, K., Kirtane, B., Jackson, J.G., Ikeno, Y., Ikeda, T., Hawks, C., Smith, J.R., Matzuk, M.M. & Pereira-Smith, O.M. (2005a) MRG15 regulates embryonic development and cell proliferation. *Mol. Cell. Biol.* **25**, 2924–2937.
- Tominaga, K., Leung, J. K., Rookard, P., Echigo, J., Smith, J.R. & Pereira-Smith, O.M. (2003) MRGX is a novel transcriptional regulator that exhibits activation or repression of the B-myb promoter in a cell type-dependent manner. *J. Biol. Chem.* **278**, 49618–49624.
- Tominaga, K., Matzuk, M.M. & Pereira-Smith, O.M. (2005b) MrgX is not essential for cell growth and development in the mouse. *Mol. Cell. Biol.* **25**, 4873–4880.
- Trappe, R., Buddenberg, P., Uedelhoven, J., Glaser, B., Buck, A., Engel, W. & Burfeind, P. (2002) The murine BTB/POZ zinc finger gene Znf131: predominant expression in the developing central nervous system, in adult brain, testis, and thymus. *Biochem. Biophys. Res. Commun.* **296**, 319–327.
- Tsukada, Y., Fang, J., Erdjument-Bromage, H., Warren, M.E., Borchers, C.H., Tempst, P. & Zhang, Y. (2006) Histone demethylation by a family of JmjC domain-containing proteins. *Nature* **439**, 811–816.
- Wismar, J., Loffler, T., Habtemichael, N., Vef, O., Geissen, M., Zirwes, R., Altmeyer, W., Sass, H. & Gateff, E. (1995) The *Drosophila melanogaster* tumor suppressor gene lethal(3)malignant brain tumor encodes a proline-rich protein with a novel zinc finger. *Mech. Dev.* **53**, 141–154.
- Yamane, K., Toumazou, C., Tsukada, Y., Erdjument-Bromage, H., Tempst, P., Wong, J. & Zhang, Y. (2006) JHDM2A, a JmjC-containing H3K9 demethylase, facilitates transcription activation by androgen receptor. *Cell* **125**, 483–495.
- Yochum, G.S. & Ayer, D.E. (2002) Role for the mortality factors MORF4, MRGX, and MRG15 in transcriptional repression via associations with Pfl1, mSin3A, and transducin-like enhancer of split. *Mol. Cell. Biol.* **22**, 7868–7876.
- Zhang, P., Du, J., Sun, B., Dong, X., Xu, G., Zhou, J., Huang, Q., Liu, Q., Hao, Q. & Ding, J. (2006) Structure of human MRG15 chromo domain and its binding to Lys36-methylated histone H3. *Nucleic Acid Res.* **34**, 6621–6628.

Received: 25 February 2007

Accepted: 22 March 2007

Supplementary material

The following supplementary materials are available for this article online:

Table S1 Primers used in this study

Figure S1 Nuclear localization of MRG15 and K4- or K36-methylated histone H3.

Figure S2 RBP2 is a histone H3K4-specific demethylase.

Figure S3 RBP2 knockdown results in increased H3K4 methylation at transcribed regions.

Figure S4 RBP2 or MRG15 knockdown affects H3K4 methylation at transcribed regions.